Preparation and Crystal Structure of the Deficient Perovskite $LaNiO_{2.5}$, solved from Neutron Powder Diffraction Data

José Antonio Alonso* and María Jesús Martínez-Lope
Instituto de Ciencia de Materiales de Madrid, C.S.I.C. Serrano 113, 28006 Madrid, Spain

The deficient perovskite $LaNiO_{2.5}$ has been prepared in powder form with excellent crystallinity by controlled reduction of $LaNiO_3$ with Zr metal in evacuated ampoules at 400 °C. The neutron powder diffraction pattern could be indexed in a monoclinic unit-cell corresponding to a superstructure of perovskite with dimensions $2a_0 \times 2a_0 \times 2a_0$ (a_0: lattice parameter of the ideal cubic perovskite), also observed by electron diffraction. The structure was solved from the neutron powder data. The oxygen vacancies are ordered in such a way that square-planar NiO_4 and NiO_6 octahedra alternate in the *ab* plane along the [1 1 0] direction. Both kinds of Ni polyhedra are fairly distorted and tilted in order to optimize the La–O distances, giving rise to a highly strained structure of metastable character. In fact, the compound readily takes up oxygen, above 175 °C in air, to give the much more stable $LaNiO_3$ perovskite.

The ideal ABO_3 perovskite structure consists essentially of a framework of parallel corner-sharing BO_6 octahedra, with the large A cation occupying a void of about the same size of an oxygen atom. If the radius of A is too small, the void is reduced in size by tilting of the octahedra. This effect is always associated with a reduction of the overall symmetry of the ideal 'aristotype' (unit-cell parameter $a = a_0 \approx 4$ Å).[1-3]

Another widely extended effect in perovskite oxides is the occurrence of non-stoichiometry, which very often is produced by oxygen deficiency. Oxygen vacancies in ABO_{3-x} defect perovskites are assimilated into the structure, resulting in large supercells of the aristotype.[4] The type of superstructure formed depends mainly on the nature of the B cation.

For instance, when the cation B is stable in a tetrahedral oxygen co-ordination, one of the most probable structures to be adopted in oxides of composition $ABO_{2.5}$ is the Brownmillerite structure,[5] exhibited by $Ca_2Fe_2O_5$, in which one-sixth of the oxygen sites are vacant. The vacancies become ordered in an orthorhombic supercell with parameters related to a_0 as $\sqrt{2}a_0 \times \sqrt{2}a_0 \times 4a_0$. Oxygen vacancies are ordered in such a way that there is an alternating sequence of octahedrally and tetrahedrally co-ordinated B cations.

When the oxygen vacancies become ordered in defect perovskites in which the cation A is too small, the tilting of the polyhedra gives rise to complicated superstructures, resulting from the superposition of both phenomena. The precise structure determination of these oxides by X-ray diffraction is particularly difficult since the superlattice reflections associated with the tilting of the polyhedra arise from the oxygen atoms, weak scatterers if compared to the A and B cations; hence neutron diffraction measurements are more suitable for these determinations.

This is the case of the defect perovskite $LaNiO_{2.5}$, the structure of which has been controversial for a long time. This perovskite $LaNiO_{2.5}$ (or $La_2Ni_2O_5$) is the $n = 2$ member of the homologous series $La_nNi_nO_{3n-1}$, the existence of which was first reported by Gai and Rao[6] on the basis of a thermogravimetric study of $LaNiO_3$ in air. Later, $LaNiO_{2.5}$ was isolated by Crespin and co-workers[7,8] by low-temperature reduction of $LaNiO_3$ under hydrogen. The X-ray powder diffraction pattern was reported and indexed in a monoclinic unit cell with $a = 11.068(2)$, $b = 11.168(2)$, $c = 7.824(2)$ Å and $\beta = 92.91(1)°$. The structure could not be solved from the X-ray powder diffraction pattern, but a structural model based on the Brownmillerite structure was proposed, in which Ni exhibits both tetrahedral and octahedral oxygen co-ordination.

In contradiction to this, Rao and co-workers[9] postulated a tetragonal cell ($a = 7.816$, $c = 7.468$ Å) for $LaNiO_{2.5}$, confirmed by electron diffraction, and proposed as a most likely structural model one involving the ordering of the oxygen vacancies along the [1 1 0] direction in the [0 0 1] planes of the perovskite lattice, giving rise to square-planar and octahedral co-ordination for Ni^{2+}, according to the site energy preference of Ni^{2+} for square-planar *vs.* tetrahedral co-ordination.

González-Calbet *et al.*[10] adopted this structural description but proposed, like Crespin *et al.*,[7] a monoclinic cell in which the relationship to the aristotype is $2\sqrt{2}a_0 \times 2\sqrt{2}a_0 \times 2a_0$, based on a four-fold superstructure observed by electron diffraction along the [1 1 0] direction (in the aristotype setting).

Apart from the tentative models mentioned above, the crystal structure of $LaNiO_{2.5}$ including the effects of the tilting of the Ni co-ordination polyhedra has not been reported so far, probably because of the lack of good X-ray or neutron diffraction patterns collected on well crystallized samples. The main aim of this paper is to describe the preparation of a good quality $LaNiO_{2.5}$ polycrystalline sample by an original method based on the reduction of $LaNiO_3$ with Zr as oxygen scavenger, as well as to report the true cell dimensions and crystal structure, determined from X-ray and neutron powder diffraction data.

Experimental

The compound $LaNiO_3$ was prepared by a liquid mix technique. Stoichiometric amounts of analytical grade $La(NO_3)_3 \cdot 4H_2O$ and $Ni(NO_3)_2 \cdot 6H_2O$ were dissolved in citric acid and the citrate solution was evaporated and slowly decomposed at temperatures up to 800 °C, in air, in order to eliminate all the organic materials. The black precursor powder was heated at 1000 °C under 200 bar (2×10^7 Pa) of oxygen pressure for 12 h. Then, the product was cooled at 300 °C h^{-1} to room temperature.

The compound $LaNiO_{2.5}$ was obtained by reduction of $LaNiO_3$ in the presence of Zr. About 1 g of $LaNiO_3$ was placed in the bottom of a Pyrex ampoule (12 mm diameter, 12 cm length). The same amount of powdered Zr metal, contained in an alumina crucible, was introduced into the ampoule, separated by 1 cm from the $LaNiO_3$ sample. The ampoule was

subsequently evacuated and sealed. It was heated at 400 °C for 48 h, then slowly cooled to room temperature. This procedure was repeated several times in order to obtain enough sample to perform the neutron diffraction experiment.

The products were characterized by X-ray powder diffraction (XRD). The diffraction diagrams were obtained with Cu-Kα radiation in a Siemens D-501 goniometer controlled by a DACO-MP computer, by step-scanning from 10 to 100° in 2θ, in increments of 0.05° and a counting time of 4s each step. The XRD diagram of $LaNiO_{2.5}$ was indexed with the TREOR4 program.[11]

The neutron powder diffraction diagram of $LaNiO_{2.5}$ was collected at room temperature in the multidetector DN5 diffractometer at the Siloé reactor of the Centre d'Etudes Nucléaires, Grenoble. A wavelength of 1.344 Å was selected from a Cu monochromator. The 800 detectors covered a 2θ range of 80°, from $2\theta_i$ = 10°. The counting time was 4 h, using about 6 g of sample contained in a vanadium can.

The crystal structure of $LaNiO_{2.5}$ was solved by a trial and error method, as detailed in the results section. Both X-ray and neutron diffraction patterns were analysed by the Rietveld method,[12] using the FULLPROF program[13] which is a strongly modified version of that developed by Wiles and Young.[14] FULLPROF enables both the conventional refinement of a proposed structural model as well as the matching of an observed diffraction profile without the previous knowledge of the crystal structure, excepting the approximate cell dimensions and space-group symmetry. In all cases, a pseudo-Voigt function was chosen to generate the line shape of the diffraction peaks. In the neutron refinements, the coherent scattering lengths for La, Ni and O were, respectively, 8.24, 10.3 and 5.805 fm. No regions were excluded in the refinements. In the final run the following parameters were refined: background coefficients, zero-point, half-width, pseudo-Voigt and asymmetry parameters for the peak shape; scale factor, positional and thermal isotropic factors (overall for X-ray data) and unit-cell parameters. Given the relatively poor resolution at high angles of the neutron diffractometer, the isotropic thermal parameters were refined in three constrained blocks, for La, Ni and O atoms. The x and y atomic parameters for La(1) and La(2) were defined as 1/4 or 3/4 since, while refined, they converged to very close values with large standard deviations. The maximum shift for atomic coordinates in the final refinement cycle was lower than 10^{-4}.

Electron diffraction was performed in a JEOL J5000 electron microscope equipped with a tilting rotating ±45° goniometer, operating at 200 kV. Samples were ground and suspended in n-butanol, then transferred to a holey carbon coated copper grid.

Thermal analysis was carried out in a Mettler TA3000 system equipped with a TC10 processor unit. Thermogravimetric (TG) curves were obtained in a TG50 unit, working at a heating rate of 5 °C min^{-1}, either in a reducing H_2–N_2(5:95) flow or in an air flow of 0.31 min^{-1}. About 50 mg of sample were used in each experiment.

Results

X-Ray Diffraction.—Black polycrystalline $LaNiO_3$ exhibited an excellent crystallinity in the XRD patterns, as manifested by the sharp rhombohedral splitting of the perovskite peaks shown in Fig. 1. The good quality of this material is an essential prerequisite to obtain a well crystallized reduction product. The compound $LaNiO_{2.5}$ was also obtained as a black powder, the XRD diagrams of which show a complex splitting of the perovskite reflections (Fig. 1), already described by Crespin *et al.*,[7] indicating a lowering in the symmetry of the reduced compound.

The TREOR program indexed the first 20 XRD peaks of $LaNiO_{2.5}$ in a monoclinic unit cell, with parameters a = 3.924, b = 3.898, c = 3.730 Å and β = 93.9°. The goodness of this solution is given by a rather high value of the M(20) factor,[15] of 36. These lattice parameters correspond just to a monoclinic distortion of the aristotype, with cell dimensions $a_0 \times a_0 \times a_0$. Such a small unit cell is just a sub-cell of the true superstructure, for which XRD gives no information. The indexing of the neutron diffraction pattern made it necessary to consider a monoclinic unit cell with doubled parameters along the three axes. Table 1 lists the position and intensities of the XRD reflections, indexed on the basis of the true doubled cell. Observe that the indices of all the peaks in Fig. 1 and Table 1 are even, since no superstructure reflections were present in the XRD diagram.

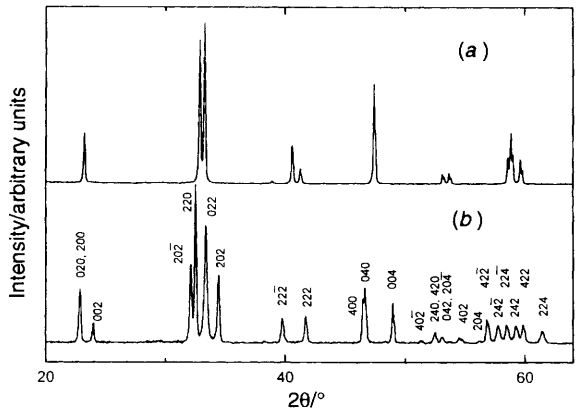

Fig. 1 The XRD diagrams for $LaNiO_3$ (a) and $LaNiO_{2.5}$ (b). For the latter, the indices of the peaks correspond to the doubled monoclinic unit cell with a = 7.8413, b = 7.7947, c = 7.4668 Å and β = 93.88°

Table 1 Miller indices, observed and calculated* d spacings and observed intensities of the peaks of the XRD pattern of $LaNiO_{2.5}$

hkl	d_{obs}	d_{calc}	I/I_0
2 0 0	3.91	3.90	35
0 2 0			
0 0 2	3.73	3.73	14
2 0 $\bar{2}$	2.791	2.794	50
2 2 0	2.760	2.761	100
0 2 2	2.693	2.693	75
2 0 2	2.609	2.611	44
2 2 $\bar{2}$	2.271	2.271	17
2 2 2	2.169	2.169	19
4 0 0	1.955	1.956	30
0 4 0	1.950	1.949	36
0 0 4	1.863	1.862	27
4 0 $\bar{2}$	1.783	1.782	4
4 2 0	1.745	1.744	9
2 4 0			
2 0 $\bar{4}$	1.728	1.727	6
0 4 2			
4 0 2	1.685	1.685	4
0 2 4	1.680	1.680	6
2 0 4	1.638	1.639	4
4 2 $\bar{2}$	1.621	1.621	17
2 4 $\bar{2}$	1.598	1.598	13
2 2 $\bar{4}$	1.580	1.579	13
2 4 2	1.562	1.562	13
4 2 2	1.548	1.547	13
2 2 4	1.511	1.511	10

* d Spacings are calculated for the unit-cell parameters refined from the XRD data, a = 7.8413(7), b = 7.7947(7), c = 7.4668(6) Å and β = 93.875(5)°, which slightly differ from those refined from the neutron data (Table 2) due to the inaccuracy of the neutron wavelength.

Neutron Diffraction.—The neutron powder diffraction pattern of $LaNiO_{2.5}$ showed a number of additional peaks arising from the ordering of the oxygen vacancies and the tilting of the NiO_n polyhedra. A doubled monoclinic $2a_0 \times 2a_0 \times 2a_0$

unit cell enabled all the additional reflections to be indexed, as shown in Fig. 2. The observed extinction conditions suggested the space group $P2_1/n$. For this crystal symmetry and unit-cell parameters the matching of the observed and calculated profiles with the FULLPROF program without a structural model led to excellent discrepancy factors. The unit-cell parameters after the final refinement of the neutron data are a = 7.8386(2), b = 7.7969(2), c = 7.4674(2) Å and β = 93.841(2)°.

With these unit-cell dimensions, a tentative structural model based on the arrangement proposed by Rao and co-workers[9] and González-Calbet *et al.*[10] was considered to solve the structure. The key point was to find out the distribution of the oxygen vacancies. From the fact that the c cell dimension is remarkably shorter than a and b it was reasonable to think that the oxygen vacancies are ordered on the ab plane, in such a way that the apical oxygens along c are missing in alternating rows of octahedra to give a vacancy stoichiometry of 0.5 per formula. A schematic projection of such a vacancy distribution is shown in Fig. 3. In order to determine the kind of tilting system of the

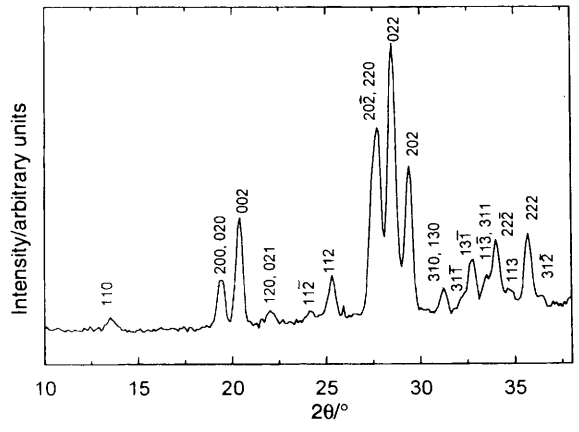

Fig. 2 Low-angle region of the neutron diffraction diagram, showing the superstructure reflections (with one or more odd Miller indices) that could not be detected by XRD

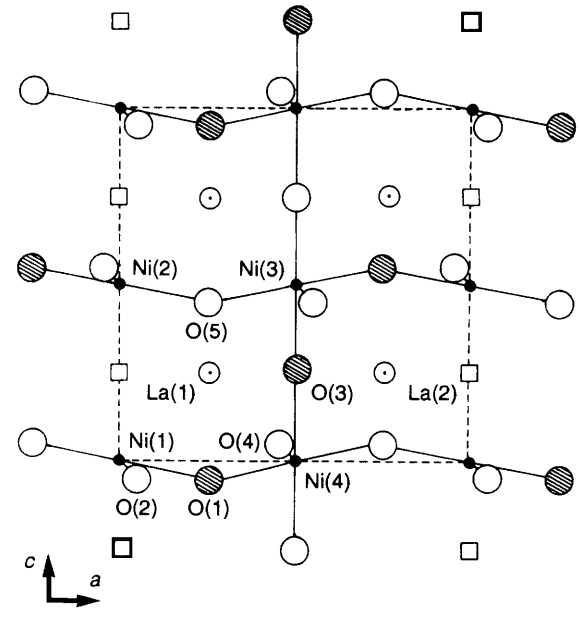

Fig. 3 Schematic representation along [0 1 0] of the $LaNiO_{2.5}$ structure, showing the ordered arrangement of the oxygen vacancies and the tilting system of the NiO_4 and NiO_6 polyhedra. Ni atoms are at height y = 0. Squares represent the oxygen vacancies. Open circles denote O atoms above the plane of the diagram while hatched circles are those below. La atoms are at heights $y = \frac{1}{4}$. The dashed line delineates the crystallographic unit cell

NiO_6 and NiO_4 polyhedra, the different hypothetical tilting models compatible with the observed lattice symmetry were built up and tried by comparing the calculated and observed neutron diffraction profiles. The only model that led to good discrepancy R factors was the one shown in Fig. 3. Table 2 includes the relevant parameters for the final refinement, and Table 3 the atomic coordinates and thermal parameters. Selected interatomic distances and angles can be found in Table 4. The agreement between the observed and calculated neutron diffraction profiles is shown in Fig. 4. The final model correctly fits the observed XRD data, leading to a Bragg R factor of 0.071. The intensities of the calculated supercell reflections for X-rays are always weaker than 1% [for instance, 0.6% for (110)], comparable to the background level.

Description of the Structure.—Two STRUPLO[16] views of the structure are shown in Fig. 5. The compound $LaNiO_{2.5}$ is a defect perovskite in which the oxygen vacancies are ordered in the ab plane along the [1 1 0] directions. The structure is constituted by NiO_6 octahedra, sharing apical oxygens along c, which alternate in the [1 1 0] directions with NiO_4 polyhedra in square-planar configuration. It contains one-dimensional chains of rather distorted NiO_6 octahedra, in which very flattened $Ni(3)O_6$ octahedra, showing extremely short Ni–O distances of 1.78 Å, alternate with elongated $Ni(4)O_6$ octahedra. Each octahedron is linked to four NiO_4 polyhedra of two kinds;

Table 2 Physical and crystallographic data and parameters for neutron powder data collection and refinement

Formula	$LaNiO_{2.5}$
M	237.605
Crystal system	Monoclinic
Space group	$P2_1/n$
a/Å	7.8386(2)
b/Å	7.7969(2)
c/Å	7.4674(2)
β/°	93.841(2)
U/Å^3	455.36(4)
Z	8
D_c/g cm^{-3}	6.93
T/K	295
λ/Å	1.344
Monochromator	Cu
Collection time/h	4
Sample weight/g	6
2θ range/°	$10.0 \leqslant 2\theta \leqslant 89.9$
2θ step/°	0.1
No. of reflections	560
Refinement	Least squares
Refined parameters	37
R_p	0.0300
R_{wp}	0.0403
R_{exp}	0.0167
χ^2	5.85
R_I	0.0344

Table 3 Atomic and thermal parameters refined from neutron powder diffraction data at 295 K for $LaNiO_{2.5}$

Atom	Site	x	y	z	B/Å^2
La(1)	4e	0.25	0.25	0.246(2)	1.0(1)
La(2)	4e	0.25	0.75	0.754(2)	1.0(1)
Ni(1)	1a	0	0	0	0.12(8)
Ni(2)	1b	0	0	0.5	0.12(8)
Ni(3)	1c	0.5	0	0.5	0.12(8)
Ni(4)	1d	0.5	0	0	0.12(8)
O(1)	4e	0.240(2)	−0.016(3)	−0.040(2)	0.18(11)
O(2)	4e	0.034(3)	0.229(3)	−0.026(2)	0.18(11)
O(3)	4e	0.500(4)	−0.047(1)	0.267(3)	0.18(11)
O(4)	4e	0.477(3)	0.265(4)	0.055(2)	0.18(11)
O(5)	4e	0.240(3)	0.050(2)	0.495(3)	0.18(11)

Table 4 Selected distances (Å) and angles (°) for $LaNiO_{2.5}$

Ni(1)–O(1)	(×2)	1.930(17)	La(1)–O(1)	2.972(22)
Ni(1)–O(2)	(×2)	1.815(23)	La(1)–O(1)	2.851(22)
Ni(2)–O(4)	(×2)	1.890(28)	La(1)–O(2)	2.561(25)
Ni(2)–O(5)	(×2)	1.920(24)	La(1)–O(2)	2.716(25)
Ni(3)–O(2)	(×2)	2.144(23)	La(1)–O(3)	2.517(29)
Ni(3)–O(3)	(×2)	1.780(24)	La(1)–O(4)	2.355(23)
Ni(3)–O(5)	(×2)	2.075(24)	La(1)–O(5)	2.434(26)
Ni(4)–O(1)	(×2)	2.042(17)	La(1)–O(5)	2.955(23)
Ni(4)–O(3)	(×2)	2.024(24)	La(2)–O(1)	2.393(21)
Ni(4)–O(4)	(×2)	2.117(28)	La(2)–O(1)	2.622(21)
			La(2)–O(2)	2.484(24)
			La(2)–O(3)	2.529(29)
			La(2)–O(4)	2.821(23)
			La(2)–O(4)	2.494(23)
			La(2)–O(5)	2.436(26)
O(1)–Ni(1)–O(2)		83.8(15)	O(1)–Ni(4)–O(3)	86.2(16)
O(1)–Ni(1)–O(2)		96.2(17)	O(1)–Ni(4)–O(4)	89.3(15)
O(4)–Ni(2)–O(5)		94.7(19)	O(1)–Ni(4)–O(4)	90.7(15)
O(4)–Ni(2)–O(5)		85.3(17)	O(3)–Ni(4)–O(4)	88.7(15)
O(2)–Ni(3)–O(3)		84.1(14)	O(3)–Ni(4)–O(4)	91.3(16)
O(2)–Ni(3)–O(3)		95.9(16)	Ni(1)–O(1)–Ni(4)	161.4(43)
O(2)–Ni(3)–O(5)		93.2(15)	Ni(1)–O(2)–Ni(3)	159.9(54)
O(2)–Ni(3)–O(5)		86.8(15)	Ni(3)–O(3)–Ni(4)	157.9(51)
O(3)–Ni(3)–O(5)		94.8(21)	Ni(2)–O(4)–Ni(4)	153.2(47)
O(3)–Ni(3)–O(5)		85.2(19)	Ni(2)–O(5)–Ni(3)	157.5(49)
O(1)–Ni(4)–O(3)		93.8(16)		

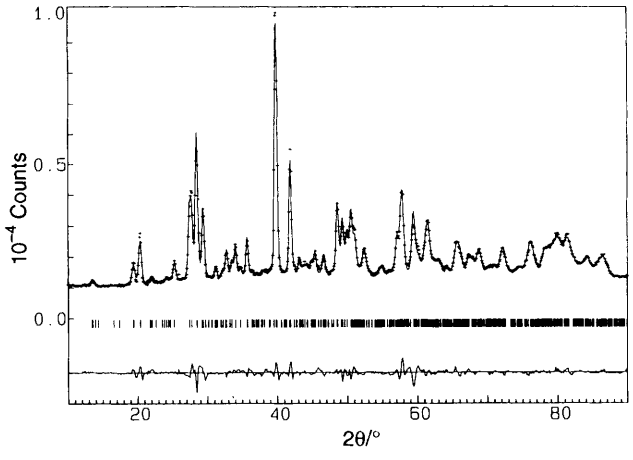

Fig. 4 Observed (crosses), calculated (full line) and difference neutron powder diffraction profiles for $LaNiO_{2.5}$ at 295 K. The vertical thin marks indicate the allowed Bragg positions

among them $Ni(1)O_4$ is also rather distorted, containing fairly short Ni(1)–O(2) bonds of 1.82(2) Å. Lanthanum atoms occupy very irregular oxygen environments, with La–O distances ranging from 2.35 to 2.97 Å.

An alternative description of the structure can be given if we consider the ideal perovskite structure as a stacking of AO and BO_2 planes along the *c* axis. Accordingly, the structure of $LaNiO_{2.5}$ can be seen as an arrangement of defect $LaO_{0.5}\square_{0.5}$ planes and NiO_2 layers along *c*, thus giving rise to square-planar and octahedral co-ordination for Ni.

Electron Diffraction.—Fig. 6 shows an electron diffraction pattern along [0 0 1], indexed on the basis of the $2a_0 \times 2a_0 \times 2a_0$ supercell determined by neutron diffraction. No additional superlattice reflections are observed along the [1 1 0] direction, which makes it unnecessary to consider the large unit cell $2\sqrt{2}a_0 \times 2\sqrt{2}a_0 \times 2a_0$ proposed previously.[7,10]

Thermal Analysis under Reducing Conditions of $LaNiO_3$.—The thermal behaviour of $LaNiO_3$ in a reducing H_2–N_2 flow is

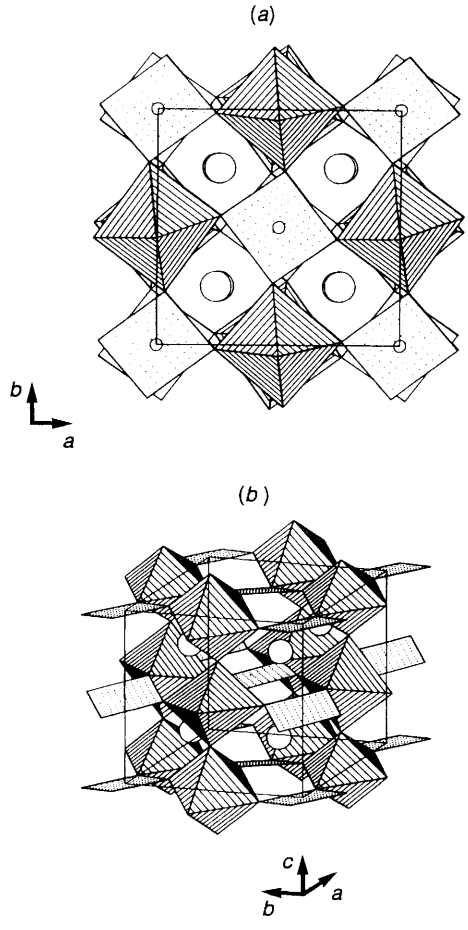

Fig. 5 Two STRUPLO[16] views of the $LaNiO_{2.5}$ structure: (*a*) projection along [0 0 1], (*b*) perspective of the unit cell. The NiO_6 octahedra (hatched) and square-planar NiO_4 (dotted) alternate in the *ab* plane, in such a way that NiO_6 octahedra form chains along the *c* axis. La atoms (open circles) are in the voids formed by the Ni polyhedra

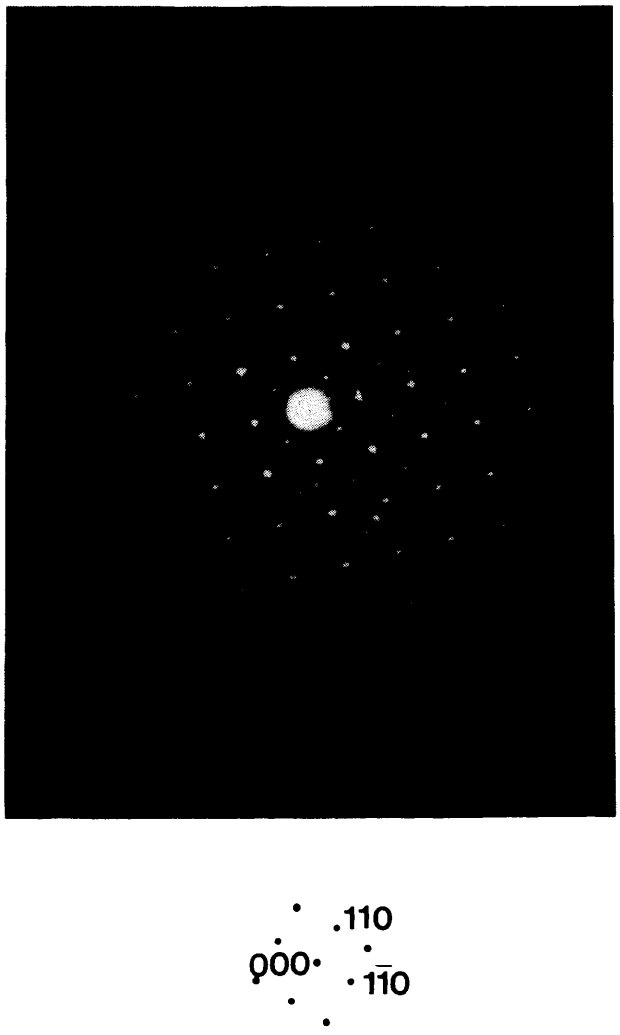

Fig. 6 Electron diffraction diagram along the zone axis [0 0 1]

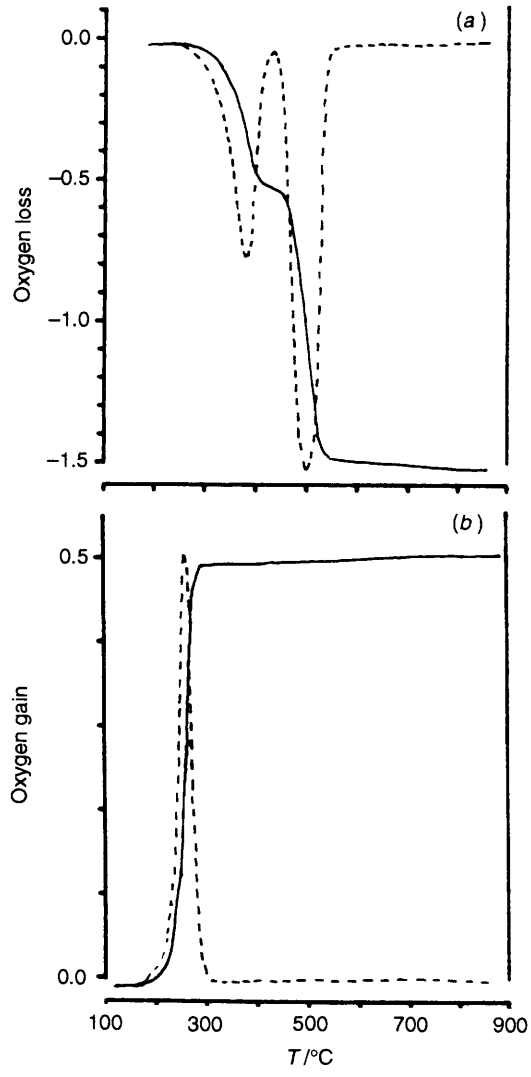

Fig. 7 The TG (solid lines) and DTG (broken lines) curves for (*a*) $LaNiO_3$, obtained in a H_2–N_2 flow, (*b*) $LaNiO_{2.5}$, obtained in an air flow

illustrated in Fig. 7(*a*). The sample is stable up to 250 °C; beyond this temperature the TG curve shows two consecutive reduction processes, with differential thermal gravimetry (DTG) temperatures centred at 390 and 510 °C. Isothermal heatings after the first reduction process enabled isolation of the intermediate single phase $RNiO_{2.5}$, showing a poorer crystallinity than that prepared by Zr reduction, as described in the experimental section. During the second step observed in the TG curve, the sample completely decomposes in a single process, also by oxygen loss, giving R_2O_3 and Ni metal as reduction products.

Reoxidation of $LaNiO_{2.5}$.The TG curve of $LaNiO_{2.5}$ in an air flow is shown in Fig. 7(*b*). The compound is stable in air up to 175 °C; above this temperature $LaNiO_{2.5}$ reabsorbs 0.5 oxygens per mol to give well crystallized $LaNiO_3$. The total reversibility of this redox process demonstrates the topotactic nature of the transformation between both perovskite-related $LaNiO_{2.5}$ and $LaNiO_3$ phases.

Discussion

The overall structure of $LaNiO_{2.5}$ basically corresponds to the model proposed by Rao and co-workers[9] and González-Calbet *et al.*:[10] the ordered arrangement of the oxygen vacancies in the solid is driven by the tendency of Ni^{2+} to adopt octahedral and square-planar co-ordination. However, the structure contains several features that must be underlined, concerning the severe distortion of the Ni co-ordination polyhedra. As shown in Table 4, the $Ni(3)O_6$ octahedron is strongly flattened along the *c* axis, and elongated along the *b* axis. The $Ni(4)O_6$ octahedron is also elongated along the *b* axis. One of the square-planar polyhedra, $Ni(1)O_4$, is elongated along the *a* axis. The presence of oxygen vacancies ordered on the *ab* plane is thought to be responsible for such distortions.

The Ni cations for which the axial co-ordination sites are vacant, *i.e.* Ni(1) and Ni(2), have correspondingly short bonds to the oxygens in equatorial positions, to compensate for the lack of the two axial Ni–O bonds. Therefore these equatorial oxygens [O(1), O(2); O(4), O(5)] which are 'overbonded' in chemical terms with Ni in square-planar co-ordination, give rise to correspondingly weak equatorial bonds to the neighbouring octahedrally co-ordinated Ni cations [Ni(3), Ni(4)]. As a further consequence, the axial Ni–O bond lengths of the octahedra become shorter along the *c* axis, especially Ni(3)–O(3). The shortening of the *c* axis must be attributed to the strengthening of the axial Ni–O bonds rather than to the ordered absence of some oxygen atoms: the direct effect of these vacancies would rather be the expansion of the lattice along *c* due to the electrical repulsion between adjacent Ni^{2+} cations.

The presence of the above mentioned very short axial bond length Ni(3)–O(3), of 1.78 Å, is, by itself, a very surprising feature of the $LaNiO_{2.5}$ structure. The sum of Shannon's ionic radii (Ni^{2+}: 0.69 Å, Ni^{3+}: 0.56 Å, O^{2-}: 1.40 Å)[17] gives an average Ni–O distance of 2.09 Å for six-co-ordinate Ni^{2+}, and 1.96 Å for

Ni^{3+}; both values are well above the observed Ni(3)–O(3) distance. Only a few nickel oxides exhibit comparatively short Ni–O distances in octahedral co-ordination, such as $BaNiO_3$ (Ni–O 1.744 Å), in which Ni is supposed to adopt an oxidation state of +4. In the family of compounds R_2BaNiO_5,[18] Ni^{2+} cations occupy the centre of flattened oxygen octahedra sharing apical corners to give one-dimensional chains, with relatively short Ni–O bond lengths of *ca.* 1.88 Å (*e.g.* Ni–O 1.881 Å in Y_2BaNiO_5). In these compounds, such short distances are the origin of strong antiferromagnetic interactions Ni–O–Ni along the chains, which behave as essentially pure one-dimensional antiferromagnetic systems.[19] In $LaNiO_{2.5}$, the presence of chains of octahedra along the *c* axis with alternating axial distances of 1.78 and 2.02 Å could suggest the existence of magnetic couplings between Ni^{2+} cations, but probably of a weak character since the Ni(3)–O(3)–Ni(4) angles, of 158°, are rather bent with respect to 180°. Very little is known about the magnetic properties of this compound. Rao and co-workers[9] reported a large magnetic susceptibility, especially at low temperatures. In our case, the magnetic measurements on the $LaNiO_{2.5}$ sample revealed the presence of very small amounts of Ni metal (less than 0.1%, undetectable by XRD and hardly visible in the neutron diffraction patterns), which masked the magnetic behaviour of $LaNiO_{2.5}$. More experimental work is needed to fully characterize this interesting deficient perovskite: low-temperature neutron diffraction studies and muon-spin relaxation measurements will be undertaken in the near future.

Conclusion

The crystal structure of $LaNiO_{2.5}$ can be considered as a monoclinic superstructure of perovskite with unit-cell dimensions $2a_0 \times 2a_0 \times 2a_0$ (a_0: lattice parameter of the ideal perovskite). It consists of an ordered arrangement of NiO_4 and NiO_6 polyhedra, in square-planar and octahedral co-ordination, respectively, with the La atoms in very asymmetrical oxygen environments. The presence of oxygen vacancies, ordered in the *ab* plane along the [1 1 0] direction, is the origin of the strengthening of the axial Ni–O bonds of the octahedra, leading to a considerable shortening of the *c* parameter with respect to *a* and *b*. The strong distortion of the Ni and La co-ordination polyhedra make the structure highly metastable, as shown by the fact that the compound readily takes up oxygen to give the much more stable $LaNiO_3$ perovskite.

Acknowledgements

The authors acknowledge the financial support of the Dirección General de Investigación Científica y Técnica to the project PB91-0089. They also thank the MDN group at the CEN, Grenoble for their hospitality and for the facilities at the Siloé reactor.

References

1 H. D. Megaw, *J. Phys. (Paris) Suppl. (C2)*, 1972, **33**, 1.
2 A. M. Glazer, *Acta Crystallogr., Sect. B*, 1972, **28**, 3384.
3 M. O'Keefe and B. Hyde, *Acta Crystallogr., Sect. B*, 1977, **33**, 3802.
4 C. N. R. Rao, J. Gopalakrishnan and K. Vidyasagar, *Indian J. Chem., Sect. A*, 1984, **23**, 265.
5 J. Berggren, *Acta Chem. Scand.*, 1971, **25**, 3616.
6 P. L. Gai and C. N. R. Rao, *Z. Naturforsch., Teil A*, 1975, **30**, 1092.
7 M. Crespin, P. Levitz and L. Gatineau, *J. Chem. Soc., Faraday Trans. 2*, 1983, 1181.
8 P. Levitz, M. Crespin and L. Gatineau., *J. Chem. Soc., Faraday Trans. 2*, 1983, **79**, 1195.
9 K. Vidyasagar, A. Reller, J. Golapakrishnan and C. N. R. Rao, *J. Chem. Soc., Chem. Commun.*, 1985, 7.
10 J. M. González-Calbet, M. J. Sayagués and M. Vallet-Regí, *Solid State Ionics*, 1989, **32/33**, 721.
11 P. E. Werner, *Z. Kristallogr.*, 1964, **120**, 375.
12 H. M. Rietveld, *J. Appl. Crystallogr.*, 1969, **2**, 65.
13 J. Rodríguez-Carvajal, FULLPROF: A Program for Rietveld Refinement and Pattern Matching Analysis, Abstracts of the Satellite Meeting of the XVth Congress of the International Union of Crystallography, Toulouse, 1990, p. 127.
14 D. B. Wiles and R. A. Young, *J. Appl. Crystallogr.*, 1981, **14**, 149.
15 P. M. de Wolff, *J. Appl. Crystallogr.*, 1968, **1**, 108.
16 R. X. Fisher, *J. Appl. Crystallogr.*, 1985, **18**, 258.
17 R. D. Shannon, *Acta Crystallogr., Sect. A*, 1976, **32**, 751.
18 E. García-Matres, J. L. Martinez, J. Rodríguez-Carvajal, J. A. Alonso, A. Salinas-Sánchez and R. Sáez-Puche, *J. Solid State Chem.*, 1993, **103**, 322.
19 J. Darriet and L. P. Regnault, *Solid State Commun.*, 1993, **86**, 409.

Received 21*st February* 1995; *Paper* 5/01036E